Dynamic Modeling of Curing Process of Epoxy Prepreg

Liangfeng Sun,[1] Su-Seng Pang,[2] Arthur M. Sterling,[1] Ioan I. Negulescu,[3] Michael A. Stubblefield[4]

[1]*Department of Chemical Engineering, Louisiana State University, Baton Rouge, Louisiana 70803*
[2]*Department of Mechanical Engineering, Louisiana State University, Baton Rouge, Louisiana 70803*
[3]*School of Human Ecology, Louisiana State University, Baton Rouge, Louisiana 70803*
[4]*Department of Mechanical Engineering, Southern University, Baton Rouge, Louisiana 70813*

Received 12 June 2001; accepted 1 November 2001

ABSTRACT: The dynamic curing process was studied by using differential scanning calorimetry (DSC) and modeled by two methods. One was based on the Kissinger and Ozawa approach, in which the activation energy was taken as a constant for all the heating rates. The whole curing process was modeled with two cure reactions. Reaction 1 exhibited the behavior of the autocatalytic reaction, whereas Reaction 2 was the *n*th order reaction. The effect of heating rate on the preexponential factor A_1 of Reaction 1 was apparent. As the heating rate increased, the A_1 decreased. There was no significant effect of heating rate on the preexponential factor A_2 of Reaction 2 and the reaction orders for both reactions. The calculated results showed that the contributions of these two reactions to the total curing process were very different and changed with the heating rate. Except in the early cure stage, the calculated total degree of cure agreed well with the experimental data. Another method was based on the Borchardt and Daniels kinetic approach, where the activation energy of the cure reaction at each heating rate was determined separately. The whole curing process was modeled with one autocatalytic reaction. The fitting results showed that both preexponential factor and activation energy increased with the increment of the heating rate. As in the first method, the effect of heating rate on the orders of reaction was very small. The calculated results agreed well with experimental values in the early cure stage. © 2002 Wiley Periodicals, Inc. J Appl Polym Sci 86: 1911–1923, 2002

Key words: curing of epoxy prepreg; kinetics; modeling; DSC

INTRODUCTION

The application of epoxy prepreg as the joints for composite pipe systems is under study.[1,2] This application involves both the dynamic and the isothermal curing process. Its kinetic properties at the different temperatures were studied and reported elsewhere.[3] The dynamic cure kinetics are very different from the isothermal cure kinetics. The rate constant is a function of temperature, so it will change during the dynamic heating process. The heating rate also affects the dynamic curing process. At the higher heating rate, the complete cure reaction could be finished in less cure time. The number of peaks and/or shoulders in the isothermal and dynamic differential scanning calorimetry (DSC) thermograms may be different.[4] Although there was only a peak in the isothermal DSC thermograms, a peak and a shoulder appeared in the dynamic DSC thermograms. The kinetic parameters obtained from an isothermal cure study are not good in predicting the dynamic cure behavior.[5] The best way to understand the dynamic curing process is through the dynamic curing experimental data.

In the isothermal curing process studied by DSC, the degree of cure was assumed proportional to the reaction heat. It was calculated either by the residual heat[6,7] or by the reaction heat at a particular time.[8–10] In the dynamic study, the degree of cure followed the same convention and was calculated in the form,

$$\alpha = \frac{\Delta H_t}{\Delta H_{\text{total}}} \tag{1}$$

where α is the degree of cure, ΔH_t is the dynamic reaction heat at time t, and ΔH_{total} is the total reaction heat at a certain heating rate.

On the basis of the resin systems, different models could be used. The first-order reaction, the *n*th order reaction, and autocatalytic reaction models have all been used to simulate the dynamic curing process.[11,12,5] The kinetic parameters, such as the preexponential factor and activation energy, could be determined either by the Kissinger and Ozawa method[13,14] or by the Borchardt and Daniels method.[15]

In this work, the dynamic curing process was studied by DSC at different heating rates. The experimen-

Correspondence to: S.-S. Pang (mepang@me.lsu.edu).
Contract grant sponsor: Louisiana Board Reagents BoR/ITRS; contract grant numbers: LEQSF(1999-02)-RD-B-10 and LEQSF(2000-03)-RD-B-05.

Journal of Applied Polymer Science, Vol. 86, 1911–1923 (2002)

tal data were modeled by autocatalytic cure kinetics. The kinetic parameters were determined by two different methods. One was based on the Kissinger and Ozawa kinetic approach. Another one was based on the Borchardt and Daniels approach.

EXPERIMENTATION

Materials

Hexcel 8552 carbon/epoxy prepreg from Hexcel Corporation, Pleasanton, California, USA, was used in this study. The carbon synthetic fiber areal weight in the prepreg tape was 137 g/m^2. The content of the multifunctional epoxy resins and the curing agent of the prepreg was 33% by weight.

Dynamic DSC method

The measurements of heat flow of the samples were conducted by using a DSC 2920 (TA Instruments Inc. New Castle, Delaware, USA). The instrument could be run in the conventional DSC mode and modulated DSC mode. In the conventional DSC mode, the dynamic scanning process was conducted at a simple constant heating rate. In the modulated DSC mode, a sinusoidal temperature profile was overlaid on a primary temperature ramp, which changed at a constant heating rate. The net effect was that the actual heating rate was sometimes greater than and sometimes less than the constant heating rate. By the modulated DSC mode, the total heat flow signal could be separated into reversal heat flow and nonreversal or kinetic heat flow.

Following the recommendation from TA Instruments, the size of the sample for the kinetic study was in the range of 5–10 mg. Considering the content of the resin in the prepreg, the size of the sample was usually 9–10 mg. Both the sample container and the reference were aluminum pans. Nitrogen was used as the purging gas. The sampling time was set to 0.2 s per point.

RESULTS AND DISCUSSION

During the dynamic measurement, the signals recorded by the instrument were based on the sample size. The amount of the sample for each measure was usually different, and the large-size samples would produce stronger signals. Therefore, it is desirable to normalize signals for the purpose of comparisons. For the heat flow to be discussed next, normalization is to 1 g. The dynamic DSC measurements were conducted at the heating rates of 2, 5, 10, 15, and 20°C/min, with the temperature ranging from 0 to 345°C. The heat flow changes measured by the conventional DSC mode during the heating process are shown in Figure 1. Figure 1(a), which shows the heat flow changes

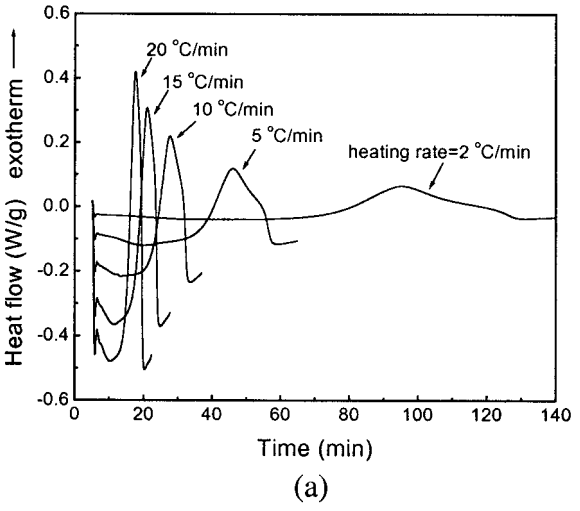

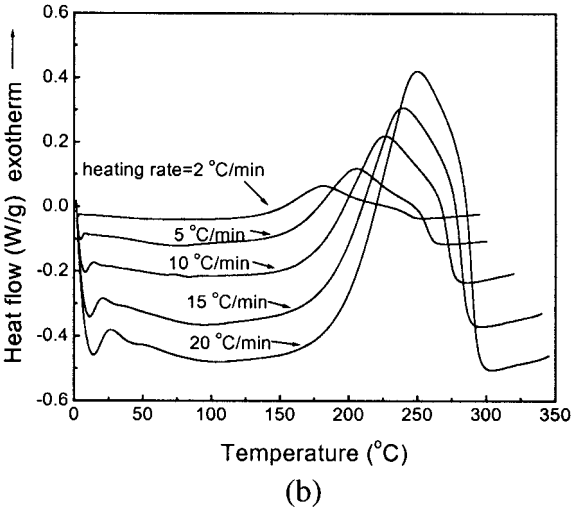

Figure 1 Heat flow changes at the heating rates of 2, 5, 10, 15, and 20°C/min: (a) from right to left by peak; (b) from left to right by peak. [(a) Heat flow versus time; (b) heat flow versus temperature.]

versus the time, was used to calculate the cure reaction heat by the method of integration. A baseline under the peak of each heat flow curve was required to determine the cure reaction heat. Two types of baselines were generally used: the straight baseline and sigmoidal baseline. The straight baseline was based on the assumption that the heat capacity changed linearly with the temperature. The sigmoidal baseline considered the possible change of heat capacity during the transition of the dynamic scanning. Dupuy et al.[12] discussed in detail the influence of the baseline on the calculations. In this study, a straight baseline was used to integrate the peak of heat flow with respect to time to give the reaction heat. Table I lists the values of the total reaction heat at each heating rate for the uncured samples. Little difference between the total reaction heats was observed at the different heating rates. The

TABLE I
Total Dynamic Cure Reaction Heat at Different Heating Rates

	Heating rate (°C/min)					
	2	5	10	15	20	Average
Heat of cure reaction (J/g)	184.8	183.4	184.2	183.9	183.7	184.0
Std error	0.2	0.9	1.6	2.2	0.9	1.2

cure reaction at each heating rate could be considered complete. Unlike the isothermal curing process controlled by diffusion,[16] the diffusion control had no effect on the dynamic curing process. The averaged cure reaction heat was 184.0 J/g. Once the reaction heat at each time or temperature and the total reaction heat at each heating rate were determined, the degree of cure α at each time or temperature could be calculated by eq. (1). By differentiating the degree of cure α with respect to time, the relationship between the cure rate and time or temperature was determined. These data would be used as the source data to simulate the dynamic curing process.

Figure 1(b) shows the heat flow changes versus temperature. In Figure 1(b), it is seen that the start and ending points shifted to the higher temperatures at the higher heating rate. Accordingly, the maximum heat flow and the exothermal peak temperature also increased. At each heating rate, the heat flow curve exhibited a peak and a shoulder, which suggested the following:

- The curing process was composed of two cure reactions.
- The peak, which occurred at lower temperature, was caused by Reaction 1.
- The shoulder, which occurred at higher temperature, was caused by Reaction 2.
- Reaction 2 was more sensitive to temperature than Reaction 1. With the increment of heating rate, the heat flow at the shoulder increased faster than that at the peak, so the rate for Reaction 2 increased faster than the rate for Reaction 1.

Further experiments with the partially cured samples in the modulated DSC mode supported the above conclusions. In the modulated DSC mode, the nonreversal heat flow that is caused by the cure reaction only was separated from the general heat flow of the curing process. The partially cured samples were prepared in a specially designed oven. The uncured sample was put into the oven and heated from room temperature to the desired temperature at a constant heating rate of 5°C/min with nitrogen as the purging gas. After the oven reached the desired temperature, the sample was quickly moved into the refrigerator and cooled in a sealed jar. The samples were partially cured to 170, 190, 200, 210, 220, 230, 240, and 270°C, separately.

The nonreversal heat flows versus temperature are shown in Figure 2. The values on the left of each corresponding peak are the exothermal peak temperature, and in parentheses, the cure temperature and degree of cure. The sample cured to 270°C had no peak. This indicated that the sample was completely cured when cured to 270°C. For all other samples, their exothermal peak temperatures could be divided into two categories: those around the lower temperature of 205°C (the first peak) and those around the higher temperature of 236°C (the second peak). The regions around the first peak were dominated by Reaction 1. All of the shoulders caused by Reaction 2 occurred after the peaks. Sample cured up to 190°C (17% cured) showed no significant change of the exothermal peak temperature, so the effect of the second reaction to the first peak was small. However, when the sample was cured to 200°C (29% cured), its peak temperature was shifted to 209°C, so the effect of the second reaction on the first peak was apparent. The regions around the second peaks were dominated by Reaction 2. When the sample was cured to 210°C (45%

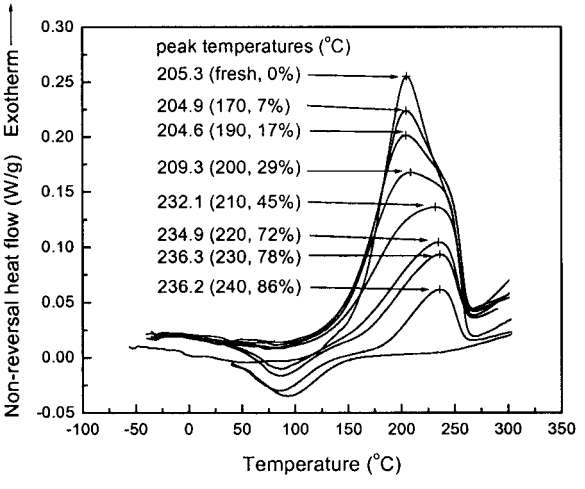

Figure 2 Nonreversal heat flow as a function of temperature for samples partially cured to, from top to bottom by peak, uncured, 170, 190, 200, 210, 220, 230, 240, and 270°C, at a heating rate of 5°C/min, starting from room temperature. The sample cured to 270°C had no peak. Values in parentheses are the cure temperature and degree of cure, respectively.

TABLE II
The Dependence of Peak Properties on the Heating Rates

		Heating rate (°C/min)				
		2	5	10	15	20
Peak 1	T (°C)	181.03	206.06	227.21	240.14	250.35
	α	0.4167	0.4602	0.4832	0.5022	0.5151
	$(d\alpha/dT)$ (1/K)	0.0163	0.0152	0.0145	0.0146	0.0149
Peak 2	T (°C)	218.75	235.31	248.63	256.98	262.95
	α	0.8642	0.8283	0.7696	0.7345	0.6971
	$(d\alpha/dT)$ (1/K)	0.0075	0.0097	0.0117	0.0128	0.0137

cured), the first peak disappeared. Instead, the shoulder occurred before the second peak, which began at 232°C. It was similar for the sample cured to 220°C (72% cured). The second peak temperatures for both samples were affected by Reaction 1. For the samples cured to 230°C (78% cured) and 240°C (86% cured), the second peak temperatures showed very little difference, so the effect of the first reaction to the second peak temperature could be neglected.

As shown in Figure 1(b), the first exothermal peak temperature was apparent, so it was easy to determine. However, the second peak temperature, caused by Reaction 2, occurred at the shoulder because of the effect of the first reaction. In such a case, the second exothermal peak temperature was determined as the temperature at the turning point in the shoulder region. It was reported that the Gaussian distribution was used for the peak separation.[5] The values for the first and second exothermal peak temperatures are provided in Table II.

For the dynamic curing process, the cure rate was not only a function of degree of cure, but also a function of temperature. The kinetic model for a dynamic curing process with a constant heating rate can be expressed in the following form[9]:

$$\frac{d\alpha}{dt} = k(T)f(\alpha) \tag{2}$$

where $d\alpha/dt$ is the cure rate, $k(T)$ is the rate constant (which depends on the temperature T), and $f(\alpha)$ is a function of α only. The rate constant $k(T)$ can be further expressed by the Arrhenius equation,

$$k(T) = Ae^{-(E_a/RT)} \tag{3}$$

where A is the preexponential factor, E_a is the activation energy, R is the gas constant, and T is the absolute temperature. Substituting eq. (3) into eq. (2) yields

$$\frac{d\alpha}{dt} = Ae^{-(E_a/RT)}f(\alpha) \tag{4}$$

For a dynamic curing process with constant heating rate, the temperature increased with the increment of cure time t. The relationship between $d\alpha/dt$ and $d\alpha/dT$ can be expressed as

$$\frac{d\alpha}{dt} = \left(\frac{dT}{dt}\right)\frac{d\alpha}{dT} \tag{5}$$

where dT/dt is the constant heating rate.

Substituting eq. (5) into eq. (4) and rearranging yields

$$\frac{dT}{dt} = A\left(\frac{d\alpha}{dT}\right)^{-1} f(\alpha)e^{-(E_a/RT)} \tag{6}$$

The preexponential factor A and activation energy E_a can be determined by the Kissinger and Ozawa kinetic approach.[13,14] Taking the logarithm on both sides of eq. (6) yields

$$\ln\left(\frac{dT}{dt}\right) = \ln A - \ln\left(\frac{d\alpha}{dT}\right) + \ln f(\alpha) + \left(-\frac{E_a}{R}\right)\frac{1}{T} \tag{7}$$

The term $f(\alpha)$ in eq. (7) may have different forms, depending on the cure mechanism. For the autocatalytic model with the initial cure rate of zero, the term $f(\alpha)$ may have the form[6]

$$f(\alpha) = \alpha^m(1 - \alpha)^n \tag{8}$$

Substituting eq. (8) into eq. (7) yields

$$\ln\left(\frac{dT}{dt}\right) = \ln A - \ln\left(\frac{d\alpha}{dT}\right) + \ln[\alpha^m(1 - \alpha)^n] + \left(-\frac{E_a}{R}\right)\frac{1}{T} \tag{9}$$

As discussed earlier, the peak temperature increased with the increment of heating rate. Equation (9) can be used to describe the relationship between the heating rate and exothermic peak temperature. The preexponential factor A changed with the heating rate, so the average value of the preexponential factors

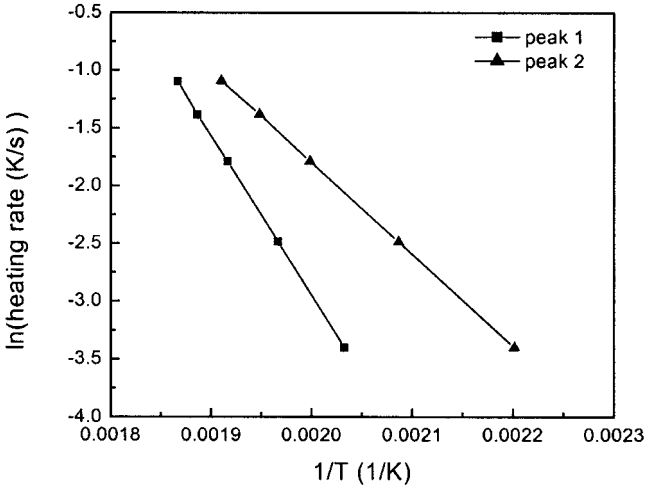

Figure 3 Plots of logarithm heating rate versus the reciprocal of the absolute exothermal peak temperature. The activation energies were determined by peak temperatures at heating rates of 2, 5, 10, 15, and 20°C/min.

at the different heating rates was used instead. Theoretically, the derivative of cure rate with respect to temperature equals zero at the peak temperature, so the derivative of degree of cure with respect to temperature ($d\alpha/dT$) at the peak temperature should be constant, regardless of the heating rate. The term $\ln[\alpha^m(1-\alpha)^n]$ at the peak temperature changed with the heating rate, but compared to term $\ln A$, its value was very small. Based on the above considerations, the general linear form between heating rate and the reversal of the peak temperature is

$$\ln\left(\frac{dT}{dt}\right) = c + \left(-\frac{E_a}{R}\right)\left(\frac{1}{T_p}\right) \tag{10}$$

where $[-(E_a/R)]$ is the slope of the curve, c is the intercept and

$$c = \ln \bar{A} - \ln\left(\frac{d\alpha}{dT}\right)_p + \ln \alpha_p^m(1-\alpha_p)^n \tag{11}$$

where $\bar{A}$ is the average value of the preexponential factors at the five heating rates. The terms T_p, $(d\alpha/dT)_p$, and α_p are the absolute temperature, derivative of degree of cure to temperature, and degree of cure at the exothermic peak, respectively. Their values are shown in Table II. It was noticed that the difference of $(d\alpha/dT)_p$ at the different heating rates was small. For peak 1, the degree of cure α_p at the peak temperature increased with the increment of heating rate. For peak 2, it was the opposite. The logarithm plots of heating rate to the reciprocal of the absolute peak temperature are given in Figure 3. It is shown that there exists a very good linear relationship between heating rate and the reversal of the exothermic peak temperature. The value for intercepts and activation energy calculated from slopes of the two peaks are given in Table III, where c_1 and E_{a1} are the intercept and activation energy for peak 1 (Reaction 1) and c_2 and E_{a2} are the intercept and activation energy for peak 2 (Reaction 2). The activation energies for Reactions 1 and 2 were 65.84 and 114.77 kJ/mol, respectively. Reaction 2 had a much higher activation energy than Reaction 1. Therefore, Reaction 2 was more sensitive to the temperature than Reaction 1. At a higher heating rate, the cure reactions shifted to a higher cure temperature range. At peak 1, which was caused mainly by Reaction 1, the total degree of cure at the higher heating rate increased due to the larger contribution from Reaction 2 at the higher cure temperature range. At peak 2, which was caused mainly by Reaction 2, the total degree of cure at the higher heating rate decreased due to the smaller contribution from Reaction 1 at the higher cure temperature range.

Based on eq. (7), a series of isoconversional plots could be obtained. In this case, each plot has the same degree of cure. At the different heating rates, the tem-

TABLE III
Dynamic Kinetics Parameters Obtained by a Method Based on the Kissinger and Ozawa Approach

		Heating rate (°C/min)				
		2	5	10	15	20
Reaction 1	A_{r1}	0.868 ± 0.001	0.698 ± 0.002	0.554 ± 0.001	0.448 ± 0.001	0.373 ± 0.001
	A_1 ($\times 10^4$ 1/s)	10.839 ± 0.514	10.004 ± 0.474	8.217 ± 0.389	7.282 ± 0.345	6.648 ± 0.315
	c_1			14.046 ± 0.0474		
	E_{a1}			65.84 ± 0.194 (kJ/mol)		
	m_1	0.546 ± 0.004	0.542 ± 0.006	0.491 ± 0.006	0.464 ± 0.007	0.474 ± 0.007
	n_1	2.461 ± 0.007	2.582 ± 0.011	2.630 ± 0.013	2.665 ± 0.015	2.675 ± 0.017
Reaction 2	A_{r2}	0.763 ± 0.002	0.894 ± 0.003	0.870 ± 0.003	0.849 ± 0.003	0.829 ± 0.003
	A_2 ($\times 10^9$ 1/s)	1.447 ± 0.151	1.712 ± 0.179	1.542 ± 0.161	1.480 ± 0.155	1.401 ± 0.146
	c_2			24.676 ± 0.105		
	E_{a2}			114.77 ± 0.45 (kJ/mol)		
	m_2	0	0	0	0	0
	n_2	0.789 ± 0.002	0.754 ± 0.003	0.724 ± 0.004	0.721 ± 0.004	0.718 ± 0.003

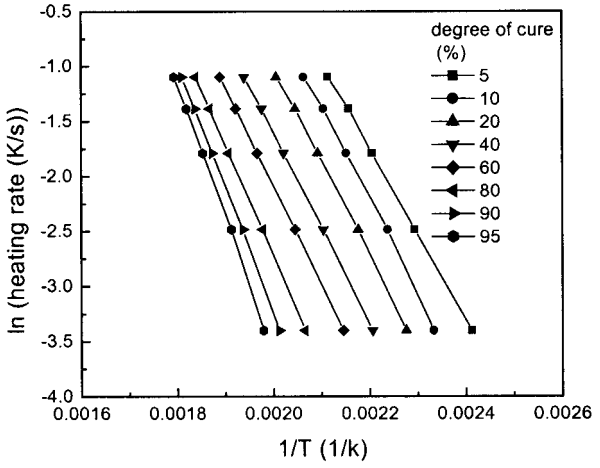

Figure 4 The isoconversional plots for logarithm heating rate versus reciprocal of the absolute temperature. The apparent activation energies were determined by isoconversional plots.

perature required to achieve the same degree of cure is different. It increased with the increment of heating rate. At each isoconversional curve, the apparent activation energy E_a should be constant. The isoconversional plots of the logarithmic heating rate versus the reciprocal of the absolute temperature are shown in Figure 4. For all the isoconversional curves, a good linear relationship is observed between the logarithm heating rate and the reciprocal of the absolute temperature. The apparent activation energy at each degree of cure is calculated from its slope in the isoconversional curve and plotted in Figure 5. The isoconversional plots helped to understand the details of the curing process. As shown in Figure 5, the apparent activation energy increased with the increment of degree of cure. At the lower degree of cure of 0.05, the apparent activation energy is close to the activation energy of the first cure reaction. At the higher degree of cure of 0.95, the apparent activation energy is close to the activation energy of the second reaction, so at the early stage of the cure reaction, the curing process was dominated by the first reaction, while at the later stage of cure reaction, the curing process was dominated by the second reaction. This assumption was further supported by the calculated results discussed next.

Equation (11) can be rearranged to obtain an expression for the average preexponential factor $\bar{A}$,

$$\bar{A} = \frac{e^c\left(\frac{d\alpha}{dT}\right)_p}{\alpha_p^m(1-\alpha_p)^n} \tag{12}$$

Having obtained the average preexponential factor $\bar{A}$ and the activation energy, we must now determine the actual preexponential factor and orders of cure reactions at each specific heating rate. To reflect the change of the preexponential factor A with the heating rate, the average preexponential factor was modified by introducing a new parameter A_r to obtain an expression for the preexponential factor A at each heating rate. If we let $A_r = A/\bar{A}$, then eq. (12) can be written as

$$A = A_r \frac{e^c\left(\frac{d\alpha}{dT}\right)_p}{\alpha_p^m(1-\alpha_p)^n} \tag{13}$$

where A_r was the correction factor of the specific preexponential factor to the average preexponential factor, which varied with the heating rate. The regression processes indicated that the introduction of A_r could greatly improve the fitting results.

Substituting eq. (8) and (13) into eq. (4) and rearranging, the final expression for the dynamic cure rate is

$$\frac{d\alpha}{dt} = A_r e^c\left(\frac{d\alpha}{dT}\right)_p e^{-(E_a/RT)} \frac{\alpha^m(1-\alpha)^n}{\alpha_p^m(1-\alpha_p)^n} \tag{14}$$

In eq. (14), the correction factor A_r and the orders of cure reaction m and n were determined by a multiple nonlinear least-squares regression method, which is based on the Levenberg–Marquardt algorithm.

As discussed earlier, two cure reactions occurred during the dynamic curing process. The contributions of these two reactions to the total reaction were not the same during the whole curing process. In the early cure stage, Reaction 1 dominated the curing process. In the later curing process, Reaction 2 dominated the curing process. The details of these two reactions can be obtained from the curve fitting results. To achieve better nonlinear fit results, the proper range of cure

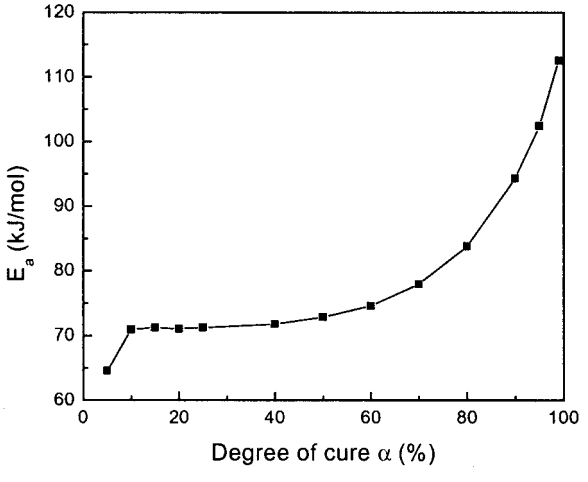

Figure 5 The activation energy, calculated by the isoconversional plots, as a function of degree of cure.

rate should be selected as the source data. Another important thing is to decide which reaction to fit first. One option was to select the early stage of cure rate as the source data to fit Reaction 1 first, then use the difference between total cure rate and fitting rate from Reaction 1 as the source data to fit Reaction 2. Another option was to select the late stage of cure rate as the source data to fit Reaction 2 first, then use the difference between total cure rate and fitting rate from Reaction 2 as the source data to fit Reaction 1. It was found that the second option achieved the better fitting results because it had a smaller residual error. Therefore, the second option was used and the range of cure rate was selected starting from about 80% degree of cure and ending with 100% degree of cure. The values for the correction factor A_r and orders of cure reaction m and n were obtained through multiple nonlinear regressions. During the regression process for Reaction 2, it was found that reaction order m_2 decreased to a very small value, about 10^{-17}, so its value was set to zero. The values of A_r, m, and n for Reactions 1 and 2 are listed in Table III, which shows the data at different heating rates along with standard errors. Reaction 1 exhibited the behavior of the autocatalytic reaction. The average values for m_1 and n_1 at the studied heating rates were 0.50 and 2.60, respectively. Reaction 2 became the nth-order reaction. The average value of reaction order at the studied heating rates was 0.74. For both reactions, it was shown that the orders of reactions changed little with the heating rate, so the effect of heating rate on the reaction orders was not significant. The averaged total reaction order of these two reactions was about 1.9 for all of the heating rates. This value was close to the reaction order of 2, which was assumed the total order of cure reaction.[6,12]

As seen in Table III, all values for A_r at the studied heating rates were less than 1, in the range of 0.868–0.373. Using eq. (13), the preexponential factor A at each heating rate was calculated and listed in Table III. Unlike the orders of reaction, the change of the preexponential factor with the heating rate for Reaction 1 was apparent. As the heating rate increased, the preexponential factor A_1 decreased. This implies that the kinetic rate constant of the same temperature for Reaction 1 decreased with the increment of the heating rate. Therefore, as the heating rate increased, the exothermal peak temperature caused by Reaction 1 shifted to the higher cure temperature. The preexponential factor for Reaction 2 showed little change with the heating rate, so the effect of heating rate on the kinetic rate constant in Reaction 2 was small.

Having obtained the kinetic parameters for these two reactions, we could calculate the values for degree of cure and cure rate for each reaction by solving the differential equations. According to eq. (4), the cure rates $d\alpha_1/dt$ of Reaction 1 and $d\alpha_2/dt$ of Reaction 2 are the function of the total degree of cure α, which equals the sum of the degree of cure α_1 by Reaction 1 and degree of cure α_2 by Reaction 2,

$$\alpha = \alpha_1 + \alpha_2 \tag{15}$$

For each reaction, substituting eqs. (5), (8), and (15) into eq. (4) and rearranging, obtains

$$\frac{d\alpha_1}{dT} = \left(\frac{dT}{dt}\right)^{-1} A_1 e^{-(E_{a1}/RT)}(\alpha_1 + \alpha_2)^{m_1}(1 - \alpha_1 - \alpha_2)^{n_1} \tag{16}$$

$$\frac{d\alpha_2}{dT} = \left(\frac{dT}{dt}\right)^{-1} A_2 e^{-(E_{a2}/RT)}(\alpha_1 + \alpha_2)^{m_2}(1 - \alpha_1 - \alpha_2)^{n_2} \tag{17}$$

where A_1, E_{a1}, m_1, and n_1 are the preexponential factor, activation energy, and reaction orders by Reaction 1, respectively, and A_2, E_{a2}, m_2, and n_2 are the preexponential factor, activation energy, and reaction orders by Reaction 2, respectively.

Equations (16) and (17) are a system of nonlinear ordinary differential equations, where the dependent variables are the degree of cure α_1 and α_2, and the independent variable is the absolute temperature T. There is no analytic solution to the above system of equations. Matlab was used to find the numerical solution. The solver used was ode45, which is based on the Runge–Kutta (4,5) algorithm. The calculated results for degree of cure α_1, α_2, and α at each heating rate are plotted in Figure 6. At different heating rates, the final contributions of reactions 1 and 2 to the total reaction were different. At a 2°C/min heating rate, the final degrees of cure for Reactions 1 and 2 were about 0.70 and 0.30, respectively, while at a 20°C/min heating rate, the final degrees of cure for Reactions 1 and 2 were about 0.38 and 0.62, respectively. With the increase of heating rate, the final degree of cure from Reaction 1 decreased. Except in the early cure stage, the calculated total degree of cure agreed well with the experimental data at all the heating rates.

Now that we have curves of degree of cure α_1, α_2, and α versus the temperature, the dependence of $d\alpha_1/dT$, $d\alpha_2/dT$, and $d\alpha/dT$ on temperature is easily obtained by differentiating the degree of cure α_1, α_2, and α with respect to temperature T. By eq. (5), the cure rates $d\alpha_1/dt$, $d\alpha_2/dt$, and $d\alpha/dt$ versus temperature T could be calculated. The plots are given in Figure 7. It is shown that the maximum cure rates for Reactions 1 and 2 changed with heating rate. At 2°C/min heating rate, the maximum cure rate of Reaction 1 was much higher than that of Reaction 2, whereas at 20°C/min heating rate, the maximum cure rate of Reaction 1 was much lower than that of Reaction 2. Increasing the heating rate increases the maximum cure rates for both reactions, but the maxi-

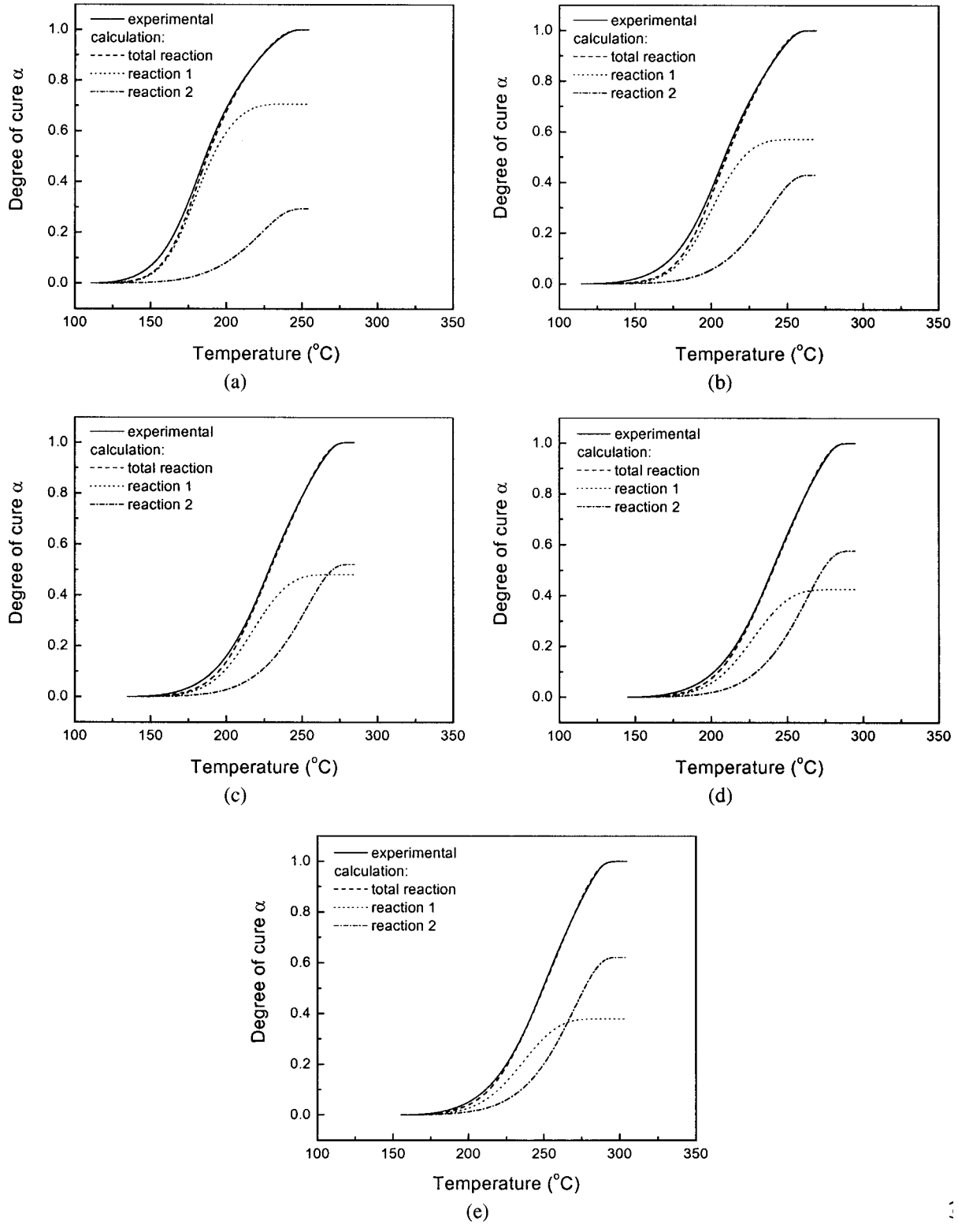

Figure 6 The degree of cure as a function of temperature calculated by a method based on the Kissinger and Ozawa approach and its comparison to the experimental value. (a) Heating rate: 2°C/min; (b) heating rate: 5°C/min; (c) heating rate: 10°C/min; (d) heating rate: 15°C/min; (e) heating rate: 20°C/min.

mum cure rate of Reaction 2 increased much faster than that of Reaction 1. The curve for the calculated total cure rate successfully predicted one peak and one shoulder in the curing process.

In the previous section, the curing process was modeled with two autocatalytic cure reactions. The preexponent factor and activation energy for each reaction were determined first by the characteristics of

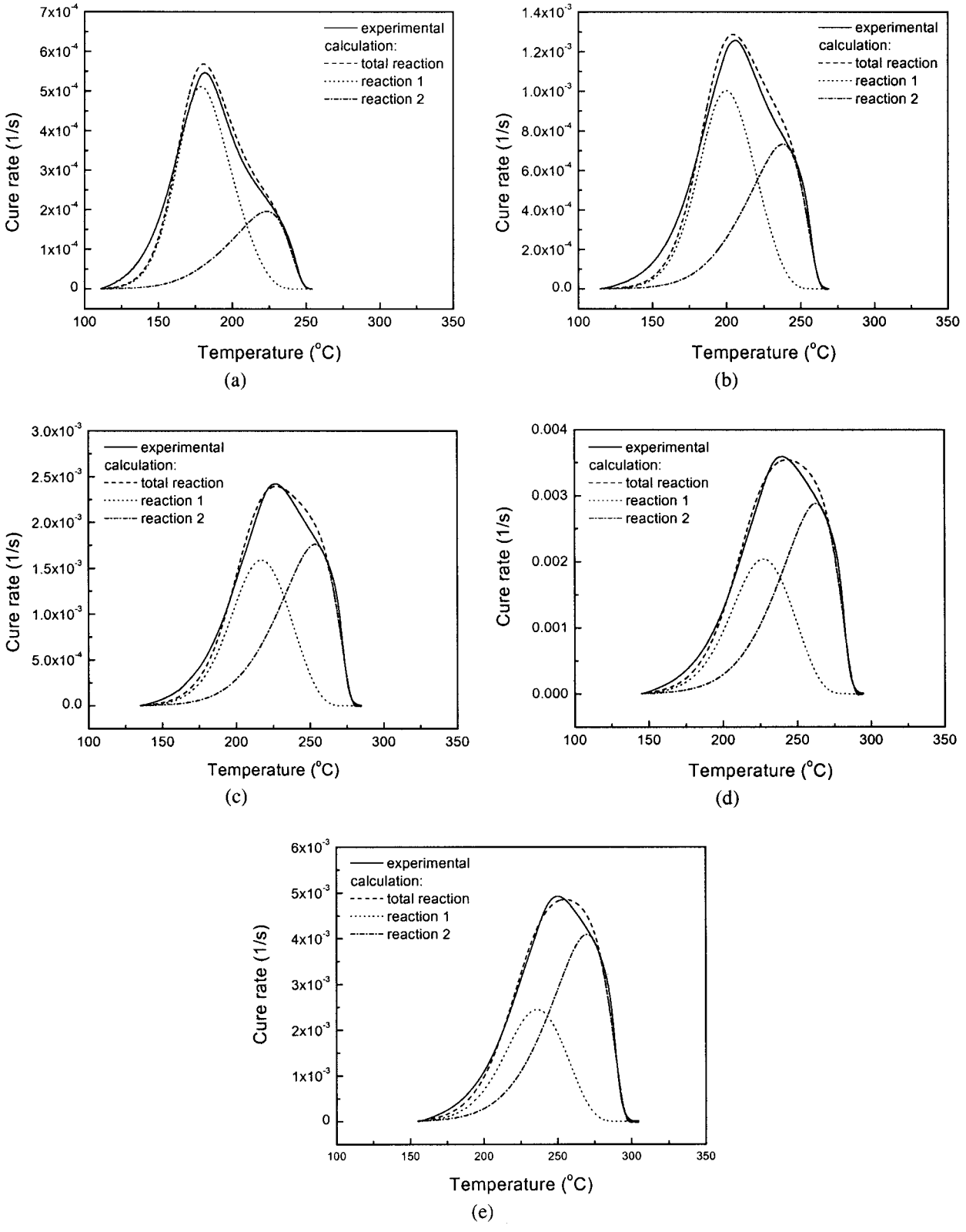

Figure 7 Cure rate as a function of temperature calculated by the method based on the Kissinger and Ozawa approach and its comparison to the experimental value. (a) Heating rate: 2°C/min; (b) heating rate: 5°C/min; (c) heating rate: 10°C/min; (d) heating rate: 15°C/min; (e) heating rate: 20°C/min.

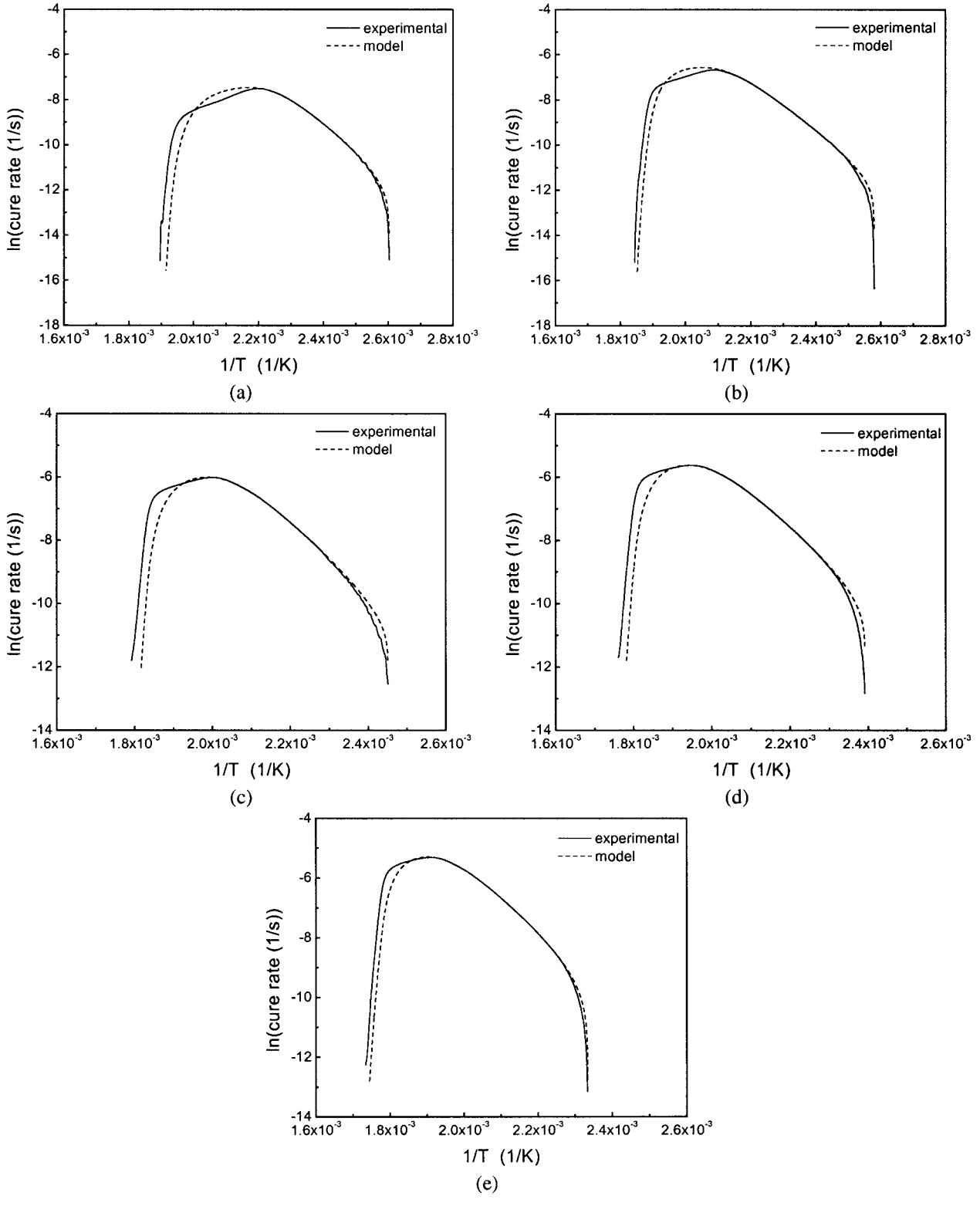

Figure 8 The modeling of logarithm cure rate versus the reciprocal of the absolute temperature compared to the experimental values. (a) Heating rate: 2°C/min; (b) heating rate: 5°C/min; (c) heating rate: 10°C/min; (d) heating rate: 15°C/min; (e) heating rate: 20°C/min.

the peaks at the different heating rates. The cure reaction orders were then determined by the multiple regressions. The whole modeling process was a little complicated. In this section, the whole curing process is studied with one autocatalytic cure reaction. The preexponent factor and activation energy for the reac-

TABLE IV
The Apparent Dynamic Kinetic Parameters Obtained by the Method Based on Borchardt and Daniels Approach

	Heating rate (°C/min)				
	2	5	10	15	20
A ($\times 10^5$ 1/s)	1.780 ± 0.012	2.144 ± 0.013	2.170 ± 0.021	3.031 ± 0.015	4.298 ± 0.017
E_a (kJ/mol)	69.93 ± 0.023	71.52 ± 0.021	71.82 ± 0.039	73.46 ± 0.019	74.99 ± 0.016
m	0.281 ± 0.005	0.216 ± 0.004	0.217 ± 0.012	0.202 ± 0.004	0.220 ± 0.005
n	1.499 ± 0.013	1.238 ± 0.013	1.338 ± 0.019	1.267 ± 0.007	1.247 ± 0.009

tion are now called the apparent preexponent factor and activation energy. Contrary to the previous method, all four parameters can be determined at the same time by the method based on the Borchardt and Daniels kinetic approach.

Substituting eq. (8) into eq. (4) yields the autocatalytic model for the dynamic curing process

$$\frac{d\alpha}{dt} = Ae^{-(E_a/RT)}\alpha^m(1-\alpha)^n \tag{18}$$

Theoretically, eq. (18) could be solved by multiple nonlinear regressions. Because the cure rate was an exponential function of the reciprocal of the absolute temperature, it was difficult to get a good solution. The fitting results showed that large errors exist for the kinetic parameters obtained by such a method. By taking the logarithm of both sides of eq. (18), a linear expression for the logarithm of cure rate can be obtained,

$$\ln\left(\frac{d\alpha}{dt}\right) = \ln A + m\ln\alpha + n\ln(1-\alpha) + \left(-\frac{E_a}{R}\right)\frac{1}{T} \tag{19}$$

Equation (19) can be solved by multiple linear regression, in which the dependent variable is $\ln(d\alpha/dt)$, and the independent variables are $\ln\alpha$, $\ln(1-\alpha)$, and $1/T$.

The plots of the logarithm cure rate versus the reciprocal of the absolute temperature at the heating rates of 2, 5, 10, 15, and 20°C/min are given in Figure 8. As shown in Figure 8, only a part of the curve exhibited a linear behavior. During the fitting process, the linear part with the negative slope was selected as the source data. The multiple linear fitted results are also given in Figure 8. A large difference between the experimental and fitted value occurred at a late stage of the curing process because of the complexity of the actual dynamic cure reaction.

The reaction orders m and n obtained by the multiple linear regressions are given in Table IV. The variation of m and n with the heating rate was small. Compared to the average values of 0.25 and 1.67 for m and n previously obtained, the average values for m and n by this method were 0.23 and 1.32, respectively. It is noticed that the reaction orders m and n had small standard errors. However, the apparent preexponential factor A and activation energy E_a had large standard errors (not shown in Table IV). Especially for A, the standard error was in the range of 10–30%. Therefore, it is necessary to redetermine the apparent preexponential factor A and activation energy E_a to reduce the magnitudes of the standard errors. Once the orders of cure reaction m and n are determined, the apparent preexponential factor A and activation energy E_a can be determined with small standard errors by the Barett method.[17] Equation (18) can be rearranged to yield

$$\frac{\left(\frac{d\alpha}{dt}\right)}{\alpha^m(1-\alpha)^n} = Ae^{-(E_a/RT)} \tag{20}$$

If there is a linear relationship between the logarithm of $(d\alpha/dt)/[\alpha^m(1-\alpha)^n]$ and $1/T$, the apparent preexponential factor A and activation energy E_a could be determined from the intercept and slope of line obtained from eq. (20). The plots of $\ln((d\alpha/dt)/[\alpha^m(1-\alpha)^n])$ versus $1/T$ are shown in Figure 9. It was noticed that a main portion of the curve exhibits a linear behavior. By fitting to the linear part of the curve, the apparent preexponential factor A and activation energy E_a were determined. Their values, with standard errors, are given in Table IV. Both the apparent preexponential factor A and the activation energy E_a were increased with the increment of the heating rates. It was noticed that the standard errors for A and E_a were greatly reduced. Therefore, values for A and E_a were more reliable. The values for the apparent preexponential factor A and the apparent activation energy E_a were greater than that of the first reaction, but less than that of the second reaction, which was discussed in the method based on the Kissinger and Ozawa approach.

With all of the kinetic parameters in eq. (18) known, the degree of cure can be calculated by solving the differential equation. Substitution of eq. (5) into eq. (18) and rearrangement yields the ordinary differential equation

$$\frac{d\alpha}{dT} = \left(\frac{dT}{dt}\right)^{-1} Ae^{-(E_a/RT)}\alpha^m(1-\alpha)^n \tag{21}$$

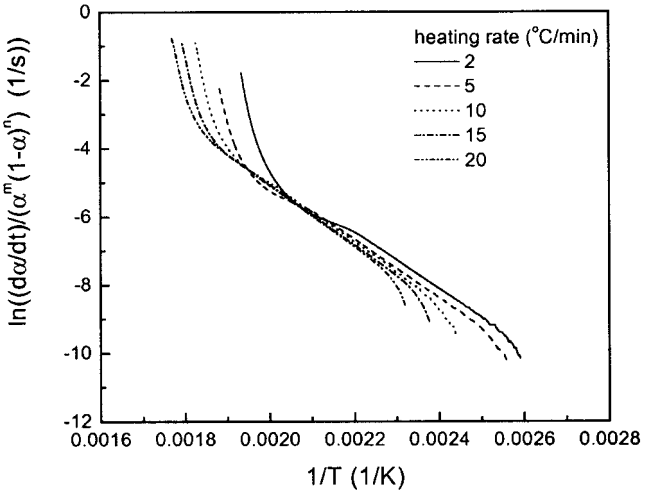

Figure 9 Plots of logarithm $(d\alpha/dt)/[\alpha^m(1-\alpha)^n]$ versus the reciprocal of absolute temperature at heating rates of 2, 5, 10, 15, and 20°C/min from right to left, respectively. The apparent preexponents and activation energies were determined from the intercepts and slopes of the linear parts of the curves.

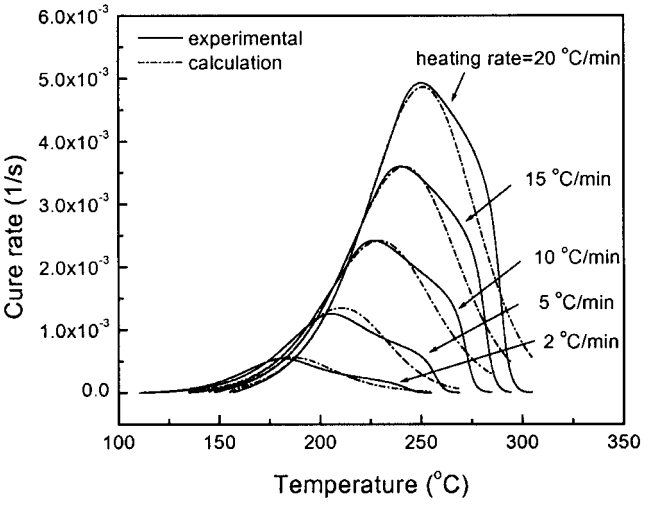

Figure 11 Cure rate as a function of temperature calculated by the method based on the Borchardt and Daniels approach at heating rates of 2, 5, 10, 15, and 20°C/min from left to right by peak and its comparison to the experimental value.

where the dependent variable is degree of cure α, and the independent variable is the absolute temperature T.

Equation (21) has no analytical solution. Matlab was used again to find the numerical solution. The calculated results at heating rates of 2, 5, 10, 15, and 20°C/min are plotted in Figure 10. At up to 0.8 degree of cure, the calculated results offered very good agreement with the experimental value. It was also noticed that the curves shifted to higher temperature ranges with the increment of heating rate. By differentiating the degree of cure α with respect to the absolute temperature T, the cure rate $d\alpha/dt$ could be obtained by eq. (5). The plots of calculated cure rate $d\alpha/dt$ versus the absolute temperature are given in Figure 11. At each heating rate, the calculated bell-shaped curve successfully predicted the peak of cure rate, especially at higher heating rates, but failed to show the appearance of the shoulder as indicated by the experimental value. Therefore, this method is more appropriate to model the simple curing process involved one cure reaction.

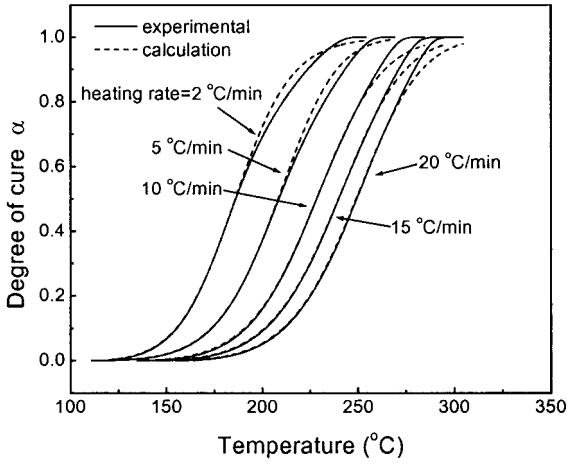

Figure 10 Degree of cure as a function of temperature calculated by the method based on the Borchardt and Daniels approach at heating rates of 2, 5, 10, 15, and 20°C/min from left to right, respectively, and its comparison to the experimental value.

CONCLUSIONS

The dynamic DSC thermograms provided much information about the curing process. The cure reaction heats at studied heating rates showed no significant difference. The whole curing process was composed of two cure reactions.

In the modeling method based on the Kissinger and Ozawa approach, the obtained activation energy and preexponential factor of the first reaction were much smaller than that of the second reaction. The reaction orders between Reaction 1 and Reaction 2 were also very different. Although the first reaction exhibited the behavior of an autocatalytic reaction, the second reaction followed the nth-order reaction model. At different heating rates, the variation of the reaction orders was very small, but the preexponential factor A_1 decreased with the increment of the heating rate. The calculated results indicated that at the early stage, Reaction 1 contributed more than Reaction 2 to the total reaction. The final contribution of Reaction 2 to the total reaction increased with the increment of heating rate. Except at the early cure stage, the calculated total degree of cure gave good prediction to the experimental value. The calculated total cure rate successfully

predicted the appearance of a peak and a shoulder in the dynamic curing process.

In the method based on the Borchardt and Daniels kinetic approach, the determined apparent preexponential factor and activation energy increased with the increment of the heating rate. The effect of the heating rate on the reaction orders was not significant. The calculated degree of cure agreed well with the experimental data in the early stage of curing process, but had a large deviance in the later stage at all of the heating rates. The calculated cure rates exhibited bell-shaped curves and failed to predict the appearance of the shoulders, so this method is more appropriate only to model the simple one-reaction curing process.

This investigation was partially sponsored by the Louisiana Board Regents BoR/ITRS program under contract numbers LEQSF(1999-02)-RD-B-10 and LEQSF(2000-03)-RD-B-05.

References

1. Stubblefield, M. A.; Yang, C.; Pang, S.-S.; Lea, R. H. Polym Eng Sci 1998, 38, 143.
2. Mensah, P. F.; Stubblefield, M. A.; Pang, S.-S.; Wingard, D. Polym Eng Sci 1999, 39, 778.
3. Sun, L.; Pang, S.-S.; Sterling, A. M.; Negulescu, I. I.; Stubblefield, M. A. J Appl Polym Sci 2002, 83, 1074.
4. Kenny, J. M.; Trivisano, A.; Berglund, L. A. SAMPE J 1991, 27, 39.
5. Karkanas, P. I.; Partridge, I. K. J Appl Polym Sci 2000, 77, 1419.
6. Yang, F.; Yao, K. D.; Koh, W. J Appl Polym Sci 1999, 73, 1501.
7. Ahn, K. J.; Peterson, L.; Seferis, J. C.; Nowacki, D.; Zachmann, H. G. J Appl Polym Sci 1992, 45, 399.
8. Lee, C.; Wei, K. J Appl Polym Sci 2000, 77, 2139.
9. Gonis, J.; Simon, G. P.; Cook, W. D. J Appl Polym Sci 1999, 72, 1479.
10. Dusi, M. R.; Galeos, R. M.; Maximovich, M. G. J Appl Polym Sci 1985, 30, 1847.
11. Jagadeesh, K. S.; Rao, G.; Shashikiran, K.; Suvarna, S.; Ambekar, S. Y.; Saletore, M.; Biswas, C.; Rajanna, A. V. J Appl Polym Sci 2000, 77, 2097.
12. Dupuy, J.; Leroy, E.; Maazouz, A. J Appl Polym Sci 2000, 78, 2262.
13. Kissinger, H. E. Anal Chem 1957, 29, 1702.
14. Ozawa, T. J. Therm Anal 1970, 2, 301.
15. Borchardt, H. J.; Daniels, F. J. Am Chem Soc 1956, 79, 41.
16. Nunez, L.; Fraga, F.; Castro, A.; Nunez, M. R.; Villanueva, M. J Appl Polym Sci 2000, 77, 2285.
17. Riccardi, C. C.; Adabbo, H. E.; Williams, R. J. J. J Appl Polym Sci 1984, 29, 2481.